

# Numerical Simulation of Core Gas Defects in Steel Castings

L. Xue

Flow Science, Inc., Santa Fe, New Mexico

M.C. Carter

Flow Science, Inc., Santa Fe, New Mexico

A.V. Catalina

Caterpillar Inc., Peoria, Illinois

Z. Lin

Caterpillar Inc., Peoria, Illinois

C. Li

Caterpillar Inc., Champaign, Illinois

C. Qiu

Caterpillar Inc., Peoria, Illinois

Copyright 2014 American Foundry Society

## ABSTRACT

Porosity is a common but serious casting defect. One type of porosity is a result of core gas that has evolved and been trapped in the casting during solidification. In order to reduce or eliminate core gas related defects, detailed information regarding the core gas generation, flow, and venting in the core, and the metal flow and solidification behavior in the mold is needed. In this paper, numerical simulations are conducted based on a prototype design, which is a steel casting part from Caterpillar. The core gas in the core and the porosity defects in the casting are analyzed and discussed, and then compared with the real casting results. Using simulations to determine porosity defects can help in optimizing the design.

**Keywords:** Porosity, Core Gas Defects, Steel Castings, Numerical Simulation, PUCB

## INTRODUCTION

The gases dissolved in the liquid, either hydrogen or nitrogen in the initial liquid, or core gas decomposed from the sand core and vented to the liquid, play a major role in porosity formation in castings. For all the analytical models that have been developed to predict the porosity defects in castings, most of them are based on tracking the evolution of dissolved gases in the initial liquid<sup>1,2</sup>. Due to the complicated physics involved, it becomes very difficult to model the core

gas evolution in the castings. However, without the consideration of core gas, predictions of porosity defects are usually insufficient. For example, in a previous study<sup>3</sup>, porosity defects in a steel casting were predicted. One of the three main regions that show porosity in the actual casting is missed in the simulation. The missed porosity region in the simulation might have resulted from core gases that vented from the core. As the quality requirements of parts become more stringent, the ability to precisely predict defects, including core gas related defects, becomes more important.

In this paper, a commercial general-purpose computational fluid dynamics (CFD) software package will be used to try to predict the core gas related defects. The software used in this study can model the core gas generation, flow, and venting in the core, but it does not track the core gas evolution in the liquid metal. However, by analyzing the core gas venting, the metal flow and solidification behavior, possible core gas defects in the castings can still be extrapolated. For comparison purposes, the same castings used in the previous work mentioned above<sup>3</sup> will be used in this paper.

## THEORY

The modeling of the casting process involves a wide variety of models, such as fluid dynamics, heat transfer, and solidification. The models used in the

CFD software have some special features. Although the description of these models can be found elsewhere<sup>4,5,6</sup>, for the sake of completeness, they are still summarized here.

### SOLIDIFICATION AND MACRO-SHRINKAGE MODEL

There are two models in the software package that can be employed to predict macro-porosity formation in metals due to shrinkage. The first model involves the solution of the full system of hydrodynamic equations. As a result, the evolution of velocity and pressure in the solidifying metal can be predicted. Therefore, this model is called the Hydrodynamic, or First Principles (FP), shrinkage model. Despite being an accurate tool to study the porosity formation phenomena, the FP model may be computationally costly because at each time step the numerical algorithm involves the complete solution of momentum and energy equations. The size of the time step, controlled by various stability criteria associated with fluid flow, may also be small compared to the total solidification time of the casting. The latter may be as long as hours for large sand castings.

The other simplified shrinkage model is based on the solution of the metal and mold energy equations only. No fluid flow equations are solved by the model. Porosity is predicted by evaluating the volume of the solidification shrinkage in each isolated liquid region in the casting at each time step. This volume is then subtracted from the top of the liquid region in accordance with the amount of liquid metal available in the cells from which the fluid is removed. The “top” of a liquid region is defined by the direction of gravity. The relevance of this approach is supported by the fact that in many situations fluid flow in the solidifying metal can be ignored. Porosity formation in that case is primarily governed by metal cooling and gravity. Feeding due to gravity often occurs on a time scale much smaller than the total solidification time. This model is called Rapid Solidification Shrinkage (RSS) model. The RSS model provides a simple tool to perform quick simulations of shrinkage in complicated castings.

### MICRO-SHRINKAGE MODEL

When the solid fraction reaches a sufficiently high value for a dendritic structure to exist throughout the bulk of the metal, further liquid flow is virtually impossible without extremely high (generally unrealistic) pressure gradients. The zero flow point is called the solid fraction for rigidity, or sometimes, the critical solid fraction. For the micro-porosity

model, it is assumed that it is this last stage of solidification that accounts for micro-porosity.

Micro-porosity can only exist in a computational element containing a solid fraction exceeding the solid fraction for rigidity. The volume shrinkage,  $\Delta V$ , in an element is computed from the change in density using a conservation of mass relation,

$$(V_{old} - \Delta V)\rho_{new} = V_{old}\rho_{old} \quad \text{Eqn. 1}$$

where “old” means at the beginning of a time step and “new” means at the end of the time step. In this expression the density is evaluated in terms of the solid fraction.

It is further assumed that the mixture density is a linear function of solid fraction,  $f_s$ ,

$$\rho(f_s) = \rho_{liq} + (\rho_{sol} - \rho_{liq})f_s \quad \text{Eqn. 2}$$

where  $\rho_{liq}$  is the density at the liquidus temperature ( $f_s=0$ ) and  $\rho_{sol}$  is the density at the solidus temperature ( $f_s=1$ ). Using the above two relations, the change in shrinkage volume,  $\Delta S$ , corresponding to the change in solid fraction,  $\Delta f_s$ , is

$$\Delta S = (1 - S)(\rho_{sol} - \rho_{liq})\Delta f_s / \rho(f_s) \quad \text{Eqn. 3}$$

where  $S$  is the current micro-porosity volume fraction and  $f_s$  is the current solid fraction.

According to this expression, the maximum shrinkage porosity (volume fraction) possible is equal to  $(\rho_{sol} - \rho_{liq}) / \rho_{sol}$ . However, the maximum micro-porosity is much less since it is associated only with solidification occurring above the critical solid fraction,

$$S_{max} = \frac{(\rho_{sol} - \rho_{liq})}{\rho_{sol}} (1 - f_{crit}) \quad \text{Eqn. 4}$$

### CORE GAS MODEL

In the CFD software, the conversion of the solid binder to gas is described by the Arrhenius equation:

$$\frac{d\rho_b}{dt} = -\rho_b C_b \exp\left(-\frac{E_b}{RT}\right) \quad \text{Eqn. 5}$$

where  $\rho_b$  is the solid binder density,  $C_b$  is the decomposition rate constant, the value of which is obtained empirically,  $E_b$  is a component binding energy,  $R$  is the universal gas constant, and  $T$  is the core temperature.

The gas is considered ideal and has a fixed composition with a specific gas constant,  $R_{cg}$ . The specific gas constant can be deduced from experiments in which the gas is collected in a fixed volume apparatus and the gas pressure is measured. The specific gas constant can be computed from the total collected standard volume,  $V_{std}$ , and the initial mass of the binder,  $m_b$ , where the specific gas constant is defined as:

$$R_{cg} = \frac{p_{std} V_{std}}{T_{std} m_b} \quad \text{Eqn. 6}$$

The microscopic velocity of the gas flow through the core,  $\vec{u}_{cg}$ , is governed by the equation for flow in porous media:

$$\vec{u}_{cg} = -\frac{K}{\mu} \nabla p_{cg} \quad \text{Eqn. 7}$$

where  $K$  is the sand permeability,  $\mu_{cg}$  is the core gas viscosity and  $p_{cg}$  is the core gas pressure.

The density of the core gas simultaneously satisfies the mass transport equation and follows the ideal gas assumption as can be seen by the equations below:

$$\frac{\partial p_{cg}}{\partial t} + \nabla \cdot (\rho_{cg} \vec{u}_{cg}) = -\frac{d\rho_b}{dt} \quad \text{Eqn. 8}$$

$$p_{cg} = R_{cg} \rho_{cg} T \quad \text{Eqn. 9}$$

In these equations  $\rho_{cg}$  is the core gas density, and  $T$  is the gas temperature. Since the core gas is compressible there can be a thermal expansion and the flow of the initial gas increases in the core as the core temperature increases, even in the absence of gas sources. The temperature of the gas generated is assumed to be equal to the local core temperature. This is a good approximation because the heat capacity of the solid core material is very large compared to that of the gas. It should be noted that in this model, the effects of humidity and moisture on gas density and on gas specific energy and temperature are ignored.

The exchange of gas at boundaries of the core material is treated as boundary conditions for the core gas model. For instance, if the core surface is exposed to air, then gas may flow across the boundary in either direction depending on the pressure difference. If there is liquid metal at the core surface, then gas is allowed to pass out of the core when its pressure is greater than the pressure of the metal at that location, but no metal is allowed to enter the core. If the metal has already solidified at the

surface of the core, then no gas is allowed to flow across the boundary at that location. At core print surfaces, where a core surface is in contact with another solid part of the mold, gas does not normally flow unless channels have been cut into the mold to allow for venting. For modeling this scenario, the core gas model has an option for allowing venting at the print surfaces.

## SIMULATIONS

The geometry of the casting/riser assembly used in the simulation is shown in Fig. 1. The metal used is steel. The chemical composition of the steel is listed in Ref. 3. The pouring temperature is 1853 K. The metal is pre-filled with uniform pouring temperature to simplify the simulation. The dimensions of the casting are 0.715m x 0.22 m x 0.235 m. The weight of the casting is about 136.8 Kg.

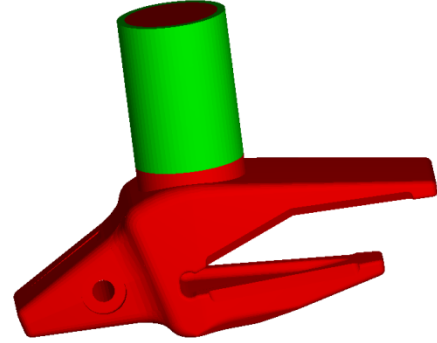


**Fig. 1. The geometry of casting/riser assembly used in the simulation**

A resin-based organic core is used. The core is a PUCB (Polyurethane Cold Box) Silica Sand core. To simulate an extreme case, no venting is allowed at the print surfaces. The grain size of the core is 180  $\mu\text{m}$  and the binder weight fraction is 1%. The binder and core gas properties used are listed in Table 1, which are taken from Ref. 5. The core and the mold have the same thermal conductivity and density\*specific heat, which are temperature dependent, and shown in Fig. 2 and Fig. 3.

**Table 1. Binder and core gas properties**

Binding energy, $E_b$ , J/mol	1.34e5
Decomposition rate, $C_b$ , 1/sec	4.25e10
Binder gas constant, $R_{cg}$ , J/kg/K	494
Binder gas viscosity, $\mu_{cg}$ , Pa·sec	1.7e-5

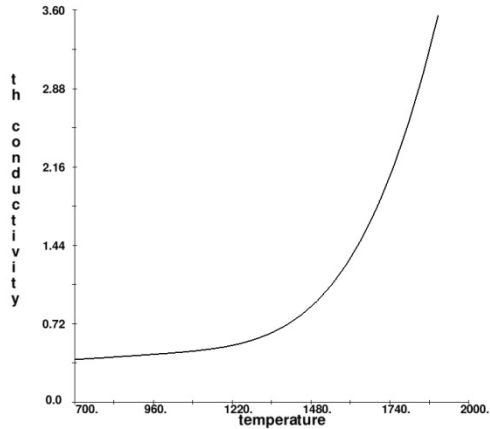


**Fig. 2. The thermal conductivity of the core/mold**

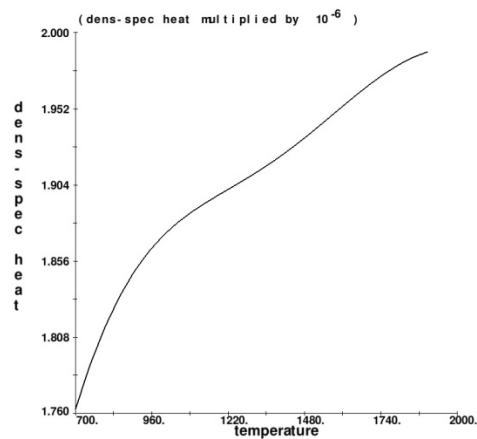


**Fig. 3. The density\*specific heat of the core/mold**

The meshed domain is 1.1m x 0.65m x 0.6m. The simulations are set to finish after all metal is solidified. To test the correctness of the parameter settings, the simulations are first run with the Rapid Solidification Shrinkage (RSS) model. Once verified, the same parameters are used to run full simulations with the First Principles (FP) shrinkage model and the core gas model. The results are then compared with the actual castings.

## RESULTS

The porosity defects in the three main porosity regions on the middle-plane longitudinal cross section of the casting are compared with Ref. 3, as shown in Fig. 4. The calculated result of the RSS model is shown in Fig. 4(b). As can be seen from the figure, the RSS model provides qualitatively satisfactory results for regions A and B, the same as reported in Ref. 3, with the benefits of fast runtimes.

The simulations are then run with the FP model and the core gas model. Notice that for RSS model, the total solidification time is about 6040 seconds, whereas for the FP model it is only about 2500 seconds. The FP model takes less time because the liquid metal convection transfers heat more efficiently. For castings with large cross sections, convective heat transfer has to be considered. If the cross sections are relatively small, the RSS model can produce good results. The micro-porosity computed by FP model is shown in Fig. 4(c).

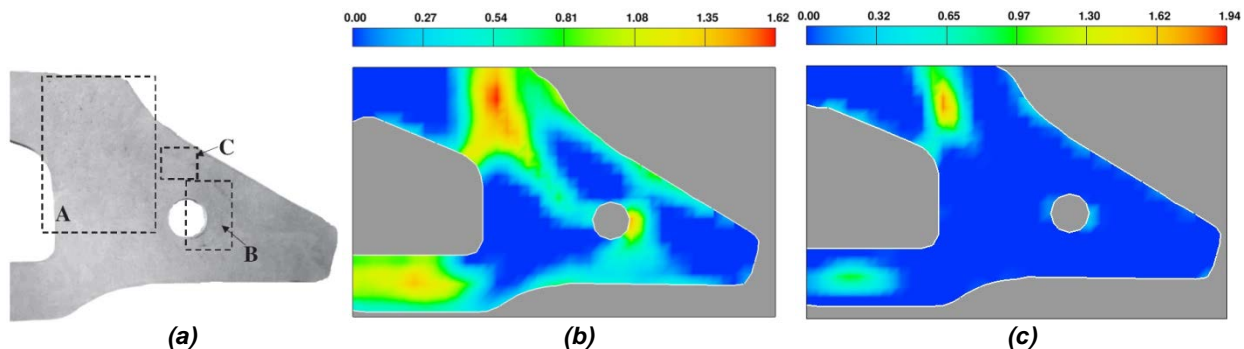


**Fig. 4. Porosity defects on the middle-plane longitudinal cross section of the steel casting. (a) Porosity defects on the test casting (Ref. 3); (b) Predicted micro-porosity (vol.%) by the RSS model; (c) Predicted micro-porosity (vol.%) by the FP model.**

As can be seen from the fig. 4(c), the FP model correctly predicts the micro-porosity in regions A and B, with a smaller porosity area than predicted by the RSS model. This is understandable considering the fluid flow in the FP model. However, like the RSS model, the FP model fails in predicting the porosity in region C. As hypothesized in Ref. 3, the porosity

in region C might have resulted from gases evolved from the core. To verify this hypothesis, the core gas surface mass flux to the metal and the metal solid fraction contour at two different times during the solidification of the FP model are plotted and shown in Fig. 5 and Fig. 6.

As shown in Fig. 5 and Fig. 6, due to the high pressure of core gas in the core, core gases vent into the metal. However, as the metal cools down, part of the core surface is sealed by the solidified metal. As the solidification front closes in, the core gases that vented to the metal at the final stages will be trapped in the metal, forming micro-porosity. As demonstrated in Fig. 5, core gases are vented to the two liquid pockets. Since the two liquid pockets are isolated by the high solid fraction region, core gases that vented to the lower liquid pocket cannot escape,

and are trapped at the solidification front, forming micro-porosity. This location coincides with the trapped location in region C. Core gases vented to the upper liquid pocket can either escape through the free surface or be trapped inside the metal, forming severe micro-porosity in the last solidified region, which is region A. Even though the core gas is not tracked explicitly in the metal, the possible locations of the porosity can still be extrapolated based on the core gas venting and metal solidification behavior.

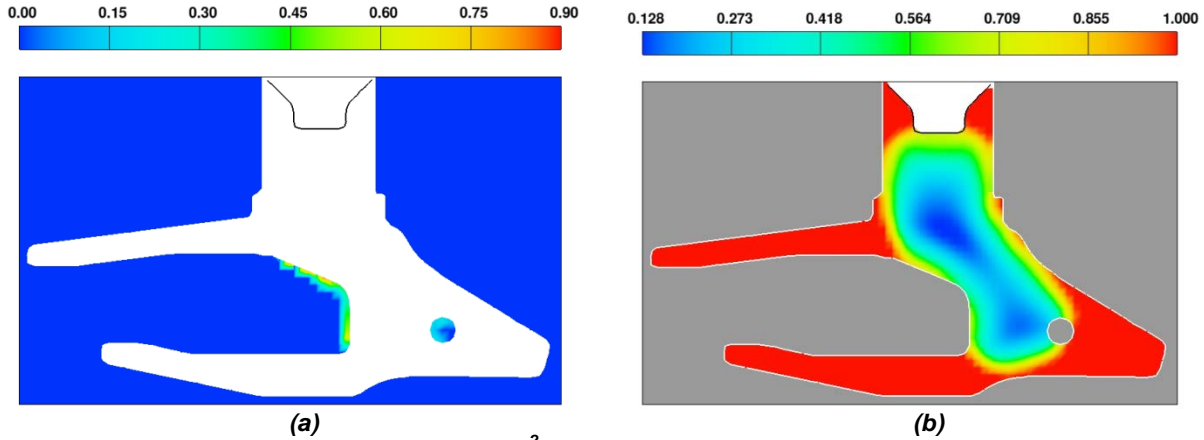


**Fig. 5. Core gas surface flux to the metal ( $kg/s/m^2$ ) and the metal solid fraction contour at  $t=1337s$ . (a) Core gas surface flux to the metal; (b) The metal solid fraction contour.**

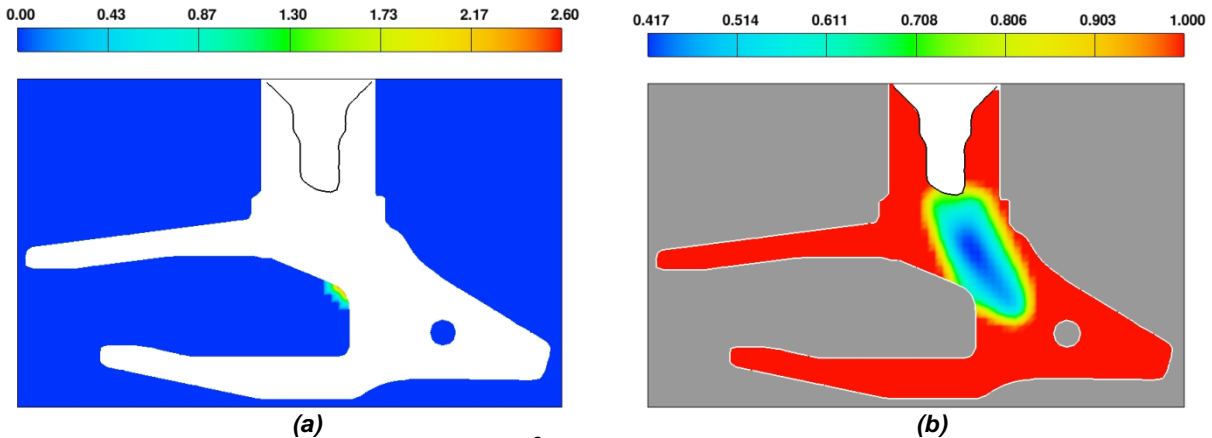


**Fig. 6. Core gas surface flux to the metal ( $kg/s/m^2$ ) and the metal solid fraction contour at  $t=2065s$ . (a) Core gas surface flux to the metal; (b) The metal solid fraction contour.**

## CONCLUSIONS

Core gases trapped in the metal is one of the important causes of the porosity in sand castings. Without the consideration of the core gases, the porosity defects predicted by numerical methods will not be complete. In this paper, simulations have been conducted in order to predict the porosity defects in a steel casting. An important porosity region is missed

without the consideration of core gases. For simulations with core gases considered, by analyzing the core gas evolution in the core and the metal solidification behavior, it is possible to determine the locations of the porosity due to core gases. Several measures can be taken to reduce the amount of core gases vented into the metal, thus reducing or eliminating the core gas porosity defects in the castings. As shown in the previous parametric study<sup>4</sup>,

adding vents, reducing the binder weight fraction, and decreasing the sand grain size are the most effective measures. The software package used in this study is a powerful tool that can be used to predict problems with core gas and study potential resolutions, enabling manufacturers to make rapid and informed changes to designs without resorting to costly experimental work.

## ACKNOWLEDGMENTS

The authors would like to thank Amanda Ruggles for her editorial help.

## REFERENCES

1. Lee, P.D., Chirazi, A., See, D., "Modeling Microporosity in Aluminum-Silicon Alloys: A Review," *J. Light Metals*, 2000, 1, 15
2. Stefanescu, D.M., "Computer Simulation of Shrinkage Related Defects in Metal Castings - A Review," *Internat. J. Cast Met. Res.*, 2005, 18, 129
3. Catalina, A.V., Leon-Torres, J.F., Stefanescu, D.M., Johnson, M.L., "Prediction of Shrinkage-Related Defects in Steel Castings," *Proceedings of the 5<sup>th</sup> Decennial International Conference on Solidification Processing, Sheffield, July 2007*
4. Carter, M.C., Xue, L., "Simulating the Parameters that Affect Core Gas Defects in Metal Castings," *Proceedings of the 117<sup>th</sup> Metalcasting Congress, St. Louis, April, 2013*
5. Starobin, A.J., Hirt, C.W., "FLOW-3D Core Gas Model: Binder Gas Generation and Transport in Sand Cores and Molds," *Santa Fe, New Mexico, USA: Flow Science Inc. TN84.*
6. Hirt, C.W., "Modeling Shrinkage Induced Micro-porosity," *Santa Fe, New Mexico, USA: Flow Science Inc. TN66.*